POLITECNICO DI TORINO
Repository ISTITUZIONALE

Controlling the melt dripping of polyester fabrics by tuning the ionic strength of polyhedral oligomeric silsesquioxane and sodium montmorillonite coatings assembled through Layer

Original
Controlling the melt dripping of polyester fabrics by tuning the ionic strength of polyhedral oligomeric silsesquioxane and sodium montmorillonite coatings assembled through Layer by Layer / Carosio, Federico; DI PIERRO, Alessandro; Alongi, Jenny; Fina, Alberto; Saracco, Guido. - In: JOURNAL OF COLLOID AND INTERFACE SCIENCE. - ISSN 0021-9797. - ELETTRONICO. - 510:(2018), pp. 142-151. [10.1016/j.jcis.2017.09.059]

Availability:
This version is available at: 11583/2688418 since: 2021-04-08T15:29:58Z

Publisher:
Academic Press Inc.

Published
DOI:10.1016/j.jcis.2017.09.059

Terms of use:

This article is made available under terms and conditions as specified in the corresponding bibliographic description in the repository

Publisher copyright

(Article begins on next page)

06 May 2024

Controlling the melt dripping of polyester fabrics by tuning the ionic strength of polyhedral oligomeric silsesquioxane and sodium montmorillonite coatings assembled through Layer by Layer

Federico Carosio[1*], Alessandro Di Pierro[1], Jenny Alongi[2], Alberto Fina[1], Guido Saracco[1]

1 Dipartimento di Scienza Applicata e Tecnologia, Politecnico di Torino, Alessandria Campus, Via Teresa Michel 5, 15121 Alessandria, Italy

2 Dipartimento di Chimica, Università degli Studi di Milano, Via Golgi 19, 20133 Milano, Italy

*Corresponding author

e-mail address: federico.carosio@polito.it

Abstract

This work deals with the Layer by Layer (LbL) assembly of hybrid organic/inorganic flame retardant coatings made of Octa-ammonium POSS (polyhedral oligomeric silsesquioxane) and sodium montmorillonite clay on polyester (PET) fabrics. The effects of ionic strength on the achieved flame retardancy properties were investigated. The coating growth as a function of different ionic strengths was evaluated by infrared spectroscopy. 0.10M NaCl was found able to promote the highest adsorption of each coating species at each deposition step strongly affecting clay stacking as evaluated by x-ray diffraction measurements. The coatings on PET assembled at high ionic strength turned out to be more homogeneous and thicker than the reference one. Thanks to the increased thickness and better surface coverage, the same coatings efficiently suppressed the melt dripping phenomenon and significantly slowed down flame spread rate in horizontal flammability tests with only 2wt% of coating mass added. Furthermore, the same performances were maintained after 1 h washing at 70°C. By cone calorimetry, coated fabrics showed a strong reduction in the combustion kinetics by nearly halving the peak of heat release rate. This paper provides an important insight on the viability of tuning deposition of LbL coatings on fabrics employing industrial-like processes by simple modification of ionic strength.

Keywords: Layer by Layer; ionic strength; POSS; sodium montmorillonite; polyester fibres; flame retardancy;

Introduction

Nowadays, synthetic fibers and fabrics, especially polyesters (PET), have become leading materials in textile industry surpassing the production of natural ones. [1] The massive use in application fields such as furniture, clothing industry, automotive amd sport equipment surrounded us with comfortable and cheap yet fast burning and melting materials. [2] The presence of such flammable materials in everyday life increases the risk of fire events in domestic scenarios. In order to prevent this occurrence, the consolidated practice is to improve the fire reaction of polymers by using chemicals known as flame retardants (FRs). FRs are normally employed in polymers either by bulk addition in melt-blending processing or, less frequently, by copolymerization of specifically designed flame retardant monomers.

In past decades, many of the effective solutions for flame retarded materials relied on the chemistry of brominated or halogenated compounds. Unfortunately, due to real or perceived health and environment hazards related to such chemicals, legislators have stimulated the research of safer alternatives. Indeed, some of the traditional FRs have been found to be toxic [3] and persistent in the environment, [4] eventually ending up in the food chain. [5] For these reasons, the research has been redirected towards the replacement of traditional chemicals with greener and safer alternatives. Within this context, a possible solution is represented by the so-called surface approach. This latter can be briefly described as a recent trend that aims at the confinement of safe flame retardants on the surface rather than in the bulk of the polymer by exploiting nanotechnology. [6, 7] This represents a change in perspective when considering the approach to fire protection and can be strictly related to the key role played by the surface during combustion. Indeed, during combustion, the heat from the flame is transmitted through the surface to the bulk; simultaneously, the bulk material thermally decomposes and produces combustible volatiles that diffuse towards the surface feeding the flame in a self-sustained process. [8] It is therefore clear that the modification of the

interface between the condensed matter and the flame may reduce heat and mass transfers hindering the combustion of a polymer. [9]

In this scenario the Layer by Layer (LbL) technique turned out to be a valuable tool for the deposition of multi-layered coatings with flame retardant functionalization on fabrics, [10] foams [11-14] and films. [15, 16] Beside flame retardancy, the LbL has been adopted in other research fields such as sensors, [17] biotechnology, [18] drug delivery control, [19] carrier systems [20], gas barrier [21] and more. [22] The LbL is a relatively simple technique; its fundamentals can be dated back to the 60's, when Iler published the experimental evidence of layered structures assembled by the alternate deposition of oppositely charged inorganic particles. [23] Later, at the beginning of the 90's, this basic concept was extended by Decher to the self-assembly of oppositely charged organic polyelectrolytes and the LbL became a general approach for the fabrication of multicomponent films on solid substrate. [24, 25] In a brief description, the LbL consists in the stepwise selective adsorption of different interacting species on a substrate. These interactions can be: electrostatic attraction, [26] hydrogen bonding, [27] ionic-covalent bonding [28] or donor-acceptor coupling. [29] All these interactions allow for the layered self-adsorption of the selected species from dilute suspensions (or solution). Following this route it is possible to obtain complex multi-layered structures with unlimited composition possibilities. Another key-point of the LbL technique, that makes this approach even more attractive, is represented by the possibility of tuning the physical/chemical characteristics of the deposited coating by changing the deposition parameters (i.e. time, concentration, pH, ionic strength, temperature). [30] However, as far as the deposition of flame retardant coatings is concerned, there are only few studies that focus on the effect of the deposition parameters on the achieved fire protection performances. Recently, we showed how pH and molecular weight of the selected polyelectrolytes can influence the burning behavior of LbL treated cotton fabrics. [31] Nevertheless, to the best of our knowledge, there are no studies evaluating the effect of ionic strength on the flame retardancy properties of the deposited LbL coatings. The ionic strength is one of the typical tuning parameter for LbL depositions; indeed, by

increasing the ionic strength it is possible to increase the film thickness and also its adhesion to the substrate. [32-34] Thereby, the optimization of ionic strength is attractive for the near-future applications of LbL as thick and highly performing FR coatings could be deposited with a reduced number of deposition steps.

In this paper, we address the deposition of a FR LbL coating consisting of octapropylammonium polyhedral oligomeric silsesquioxane (OAPOSS) and sodium montmorillonite (MMT) on PET fabrics, investigating whether tuning the ionic strength of the LbL process may improve the FR performances of the coating while maintaining a low number of deposition steps. While both OAPOSS and MMT have been previously exploited in surface approach to flame retardancy, [35, 36] their combination in a LbL assembly has never been attempted before. Moreover, the effects of the LbL deposition parameters on the achieved FR properties on synthetic fabrics have not been studied as heavily as for natural ones. The reasons have to be found in the different burning behavior of the two substrates. Indeed, differently from natural fibers, synthetic thermoplastic fibers can melt and vigorously drip during heating and combustion thus limiting the efficiency of the deposited LbL coating. This behavior poses additional and strong scientific challenges as the deposited coating has to be extremely efficient in order to obtain a substantial FR effect.

First, the coating growth at different ionic strengths has been evaluated by infrared spectroscopy. Then, the best growing conditions, along with the unmodified assembly, have been selected and applied to PET fabric employing a process similar to conventional finishing treatments, as reported in Figure 1.

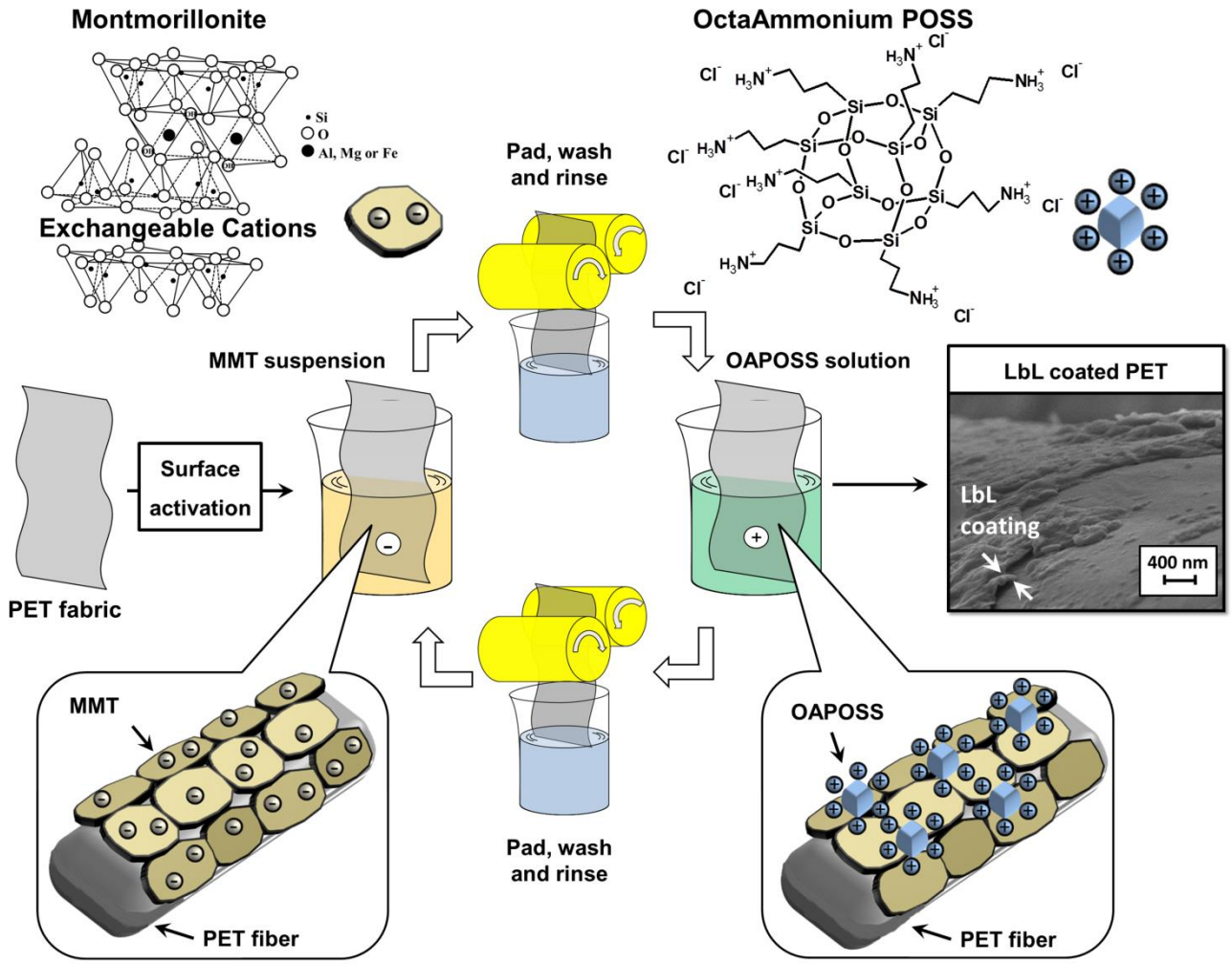

Figure 1. Schematic representation of the LbL process adopted in the present study. The PET fabric is primed by a branched poly(ethylene imine) - B-PEI - and then alternatively dipped in MMT suspension (negative) and OAPOSS solution (positive) until 5 BL are reached.

The use of such industrially-viable approach is of scientific interest and challenging at the same time. Indeed, while padding is directly relevant to industrial application, the high deformation imparted to the coating during processes might compromise the deposition of the coating to the point of making it impracticable. This is particularly important for LbL assemblies at high ionic strength since in the wet and swollen state the interactions between the components are weaker and thus the coating is more likely to suffer from strong deformations. [37]

Treated fabrics have been imaged by Field-Emission Scanning Electron Microscopy (FE-SEM) and probed by FTIR-ATR spectroscopy in order to assess the changes in fabric morphology and surface

chemical composition. The thermal and thermo-oxidative stability have been studied by thermogravimetric analyses (TGA) in nitrogen and in air, respectively. The flame retardancy properties have been evaluated by means of reaction to a small flame application (horizontal flame spread tests) and to an impinging heat flux (cone calorimetry). Finally, the best formulation has been selected for a simple washing test in order to obtain preliminary information concerning the durability of the deposited coatings.

Experimental

Materials

The polyester fabric with a *grammage* of 55 g/m^2 was purchased from Fratelli Ballesio S.r.l. (Torino, Italy). The surface was activated with an aqueous solution of 0.1 wt% of branched poly(ethylene imine) (B-PEI, Mw ~25000 g/mol by Laser Scattering, Mn ~10000 g/mol by Gel Permeation Chromatography, as reported by the Sigma Aldrich distributor). The pH of the solution was kept unaltered at pH=10. The sodium montmorillonite, MMT, Cloisite® Na^+ from Southern clays (Gonzales, TX, USA), was used for preparing 1 wt% water suspension that was kept under magnetic stirring for 24 h and then centrifuged for 5 min at 4400 rpm to remove the bigger and unsuspended particles, yielding a final concentration of 0.7 wt%. The octapropylammonium polyhedral oligomeric silsesquioxane (OAPOSS) was purchased from Hybrid Plastics (Hattiesburg, MS, USA) and solubilized at 1 wt%. This product is highly soluble in water and was used as received. The NaCl used to change the ionic strength to the aqueous solutions was purchased from Sigma Aldrich with (99.5% reagent grade) and used without further treatments. Solutions and suspensions were prepared using 18.2 MΩ deionized water supplied by a Q20 Millipore system (Milano, Italy).

LbL deposition

The coating growth at different ionic strengths has been evaluated by infrared spectroscopy on Si wafer, then, the same coating deposition procedure was replicated to PET fabrics using a padding process.

Si wafers: In order to prime the surface, the Si wafer was dipped for 2 min in the 0.1wt% B-PEI solution before the deposition cycles. This step promotes the LbL coating growth and adhesion, as previously reported in the literature. [38] Then, the growth of three different ionic strength samples on Si wafers has been monitored by using infrared spectroscopy; namely, a system made of MMT and OAPOSS without NaCl in solution and two systems with the addition of 0.05M and 0.10M of NaCl in every vessel (including the rinsing ones). After the activation step in B-PEI, the Si wafer was alternately immersed into the negatively (MMT) and the positively (OAPOSS) charged solutions (2 min dipping); after each adsorption step, the excess solution was removed by static washing (2 min) followed by flowing compressed air to remove water droplets.

PET fabrics: similarly to Si wafer, the PET fabrics were dipped 2 min in the 0.1 wt% B-PEI solution. Then, the fabrics were alternately dipped into the negatively (MMT) and the positively (OAPOSS) charged solutions (2 min dipping) following the procedure described in Figure 1. In between each adsorption step, the fabrics were squeezed using a Padder model FL300 produced by Gavazzi s.r.l (Bergamo, Italy) and dried in a convection oven at 80°C for 5 min, mimicking a finishing industrial treatment. Then, before moving to the next deposition solution the fabrics were washed in water for 2 min dipping, bearing the same ionic strength of the one employed for the deposition. The process was repeated in order to deposit a total of 5 BL, either without modifying the ionic strength or in the presence of 0.10M NaCl. The corresponding samples were coded as 5 BL and 5 BL 0.10M NaCl. The final weight gain on fabrics was approximately 1.2% and 2.0% wt. for the system untreated with NaCl and treated in the presence of 0.10M NaCl, respectively. A set of 6 samples having size 150x50 mm^2 and treated with 5 BL 0.10M NaCl has been selected for a preliminary and simple washing test to check the durability of the coating. Washing was performed

using deionized water (1 liter) at 70°C, the temperature was set using a heated magnetic stirrer and controlled using a thermocouple. The washing time was 1h, during this time the washing bath was kept under vigorous stirring using a bar magnet (length 60 mm).

Characterization

Fourier transformed-infrared spectroscopy (FT-IR): the growth of the LbL assembly on a Si wafer substrate was followed at room temperature using a FT-IR spectrophotometer in transmission mode (16 scans and 4cm^{-1} resolution, Perkin Elmer mod. Frontier, Waltham, MA, USA). IR spectra in the range 4000-400 cm^{-1} were acquired after each bilayer was built.

Fourier transformed-infrared spectroscopy in attenuated total reflectance (FT-IR ATR): spectra were collected at room temperature in the range 4000-700cm^{-1} (16 scans and 4cm^{-1} resolution) using the same FT-IR/FIR spectrophotometer cited before (Perkin Elmer mod. Frontier, Waltham, MA, USA) equipped with a germanium crystal.

Field Emission-Scanning Electron Microscopy: the surface morphology of untreated and LbL-coated fabrics was observed using a Field-Emission Scanning Electron Microscope (FE-SEM), model Merlin from Zeiss (Jena, Germany). Samples were cut in 100x100 mm^2 pieces, pinned up to conductive adhesive tapes and chrome-metallized (5-7 nm) prior to imaging.

Thermogravimetric analysis: TGA were performed on a thermogravimetric balance TGA-Q500 by TA Instruments (Laboratory for Emerging Materials and Technology, South Carolina, USA) from 50 to 800°C (using heating rate of 10°C/min) in both nitrogen and air (gas flux 60mL/min). 10±0.5 mg samples were placed in open alumina pans. From TG and dTG curves, the collected data were T_{onset} (temperature at 5% weight loss), T_{max} (temperature at maximum weight loss rate) and the residue at 800°C.

Horizontal flame spread tests: the flammability test was evaluated in horizontal configuration following the UL 94 HB testing scheme. A 45 degrees inclination along the horizontal direction has been set to allow a more realistic flame spread. The specimen (size: 150 x 50 mm^2) was ignited from its short side by a 20 mm methane flame (flame application time: 3 s). Five samples were tested for each formulation. Dry cotton was placed underneath the testing specimen. During the test, parameters such as afterflame time (time of flame persistence after the ignition source has been removed, in seconds), average burning rate (mm/s), occurrence of melt dripping, cotton ignition and final residue (%) were collected.

Cone Calorimetry: an ISO 5660 cone calorimeter from Fire Testing Technology FTT (East Grinstead, UK) was employed to investigate the forced combustion behavior of the fabrics under a specific heat flux. Specimens were wrapped in aluminum foil leaving the upper surface exposed to the cone resistance and placed on ceramic backing board at a distance of 25 mm from cone. Due to the lightweight nature of the fabric this test has been performed on 6 plies stacked-up together and hold in position with a metallic grid (wire diameter 2 mm, distance between wires 18 mm). The square samples of 6 plies 100x100mm^2 were irradiated by a heat flux of 35kW/m^2 in horizontal configuration, following the procedure previously reported elsewhere. [39] The registered parameters were: Time To Ignition (TTI, s), the Heat Release Rate (HRR and its peak pkHRR, kW/m^2), the Total Heat Release (THR, MJ/m^2), the Total Smoke Released (TSR, m^2/m^2) and final residual mass. The test was repeated 3 times for each formulation, the average results are reported. Standard deviation (σ) between results from repeated tests was calculated and taken as the experimental error for each of the mentioned parameters. Before combustion tests, specimens were conditioned at 23±1°C and 50±1% relative humidity for 48 h in a climate chamber.

Results and discussion

Coating growth by FTIR

The coating growth at different ionic strength was monitored through FT-IR on Si wafers. First of all, the spectrum of each layer constituent has been evaluated (supplementary material Figure S1). Neat OAPOSS shows characteristics peaks ascribed to Si-O-Si cage vibrations in the 1200-1000 cm^{-1} range with the most intense peak at 1132 cm^{-1} ascribed to Si-O stretching. [40] Moreover, signals related to NH_3^+ asymmetric and symmetric stretching vibrations can be found at 1612 and 1510 cm^{-1}, respectively (Figure 2a). [41] For what concerns MMT, characteristics signals are found at 1043 cm^{-1} (Si-O stretching vibration), 520 cm^{-1} (Si-O-Al bending vibration) and 464 cm^{-1} (Si-O-Si bending vibration). [42] The two components have been LbL assembled evaluating the effects of ionic strength on the coating growth. Figure 2 reports the IR signals of the OAPOSS/MMT system grown on a silicon substrate with no added salt and the intensity plot of characteristic peaks as a function of BL number for each tested salt concentrations.

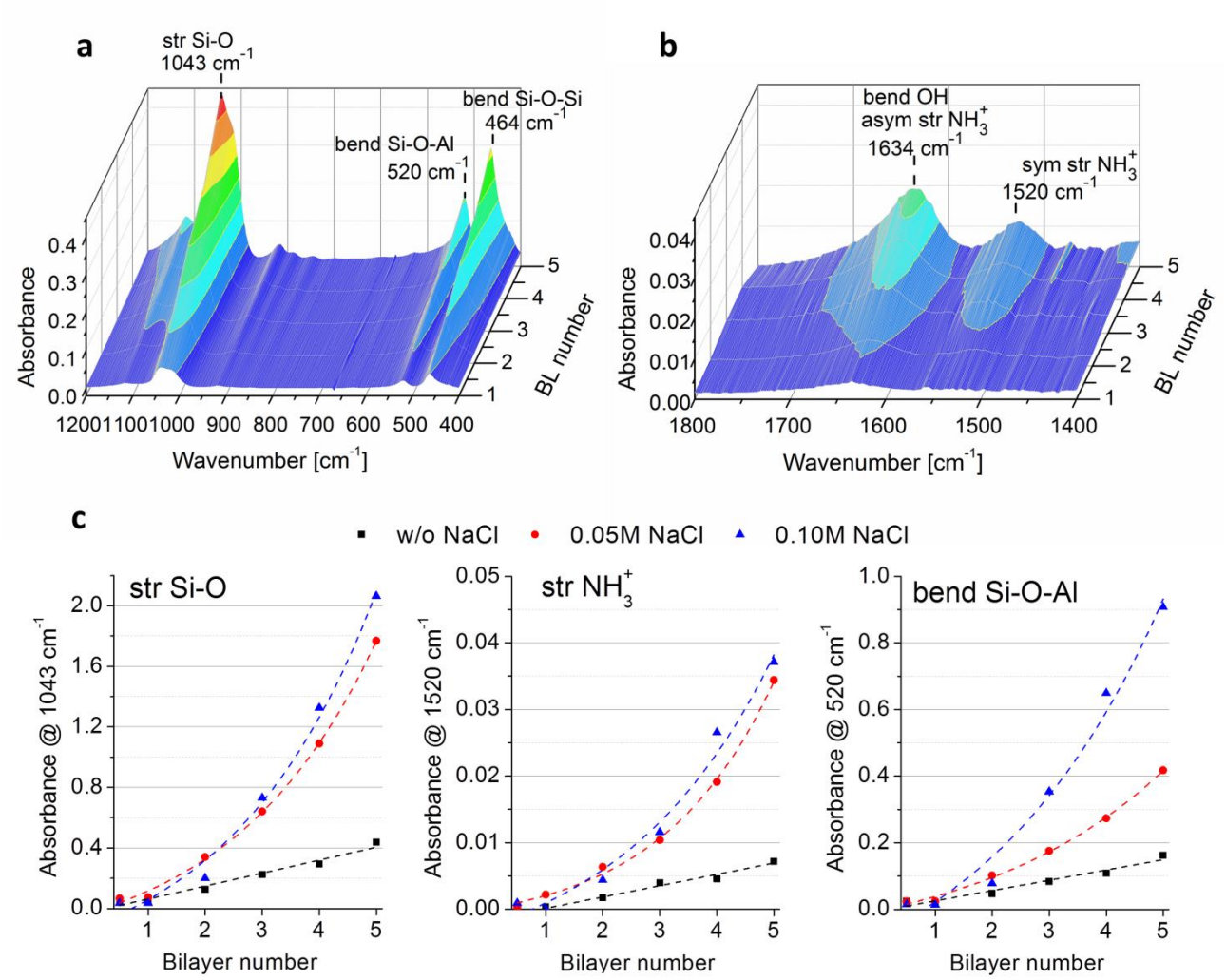

Figure 2. IR characterization of LbL assembly: 3D plot absorptions in the 1800-1400 (a) and 1200-400 cm^{-1} (b) of LbL assembled OAPOSS/MMT unmodified ionic strength and signal intensity of 1043, 1520 and 520 cm^{-1} as a function of BL number at different ionic strengths (c).

When assembled at unmodified ionic strength, *i.e.* with no added NaCl, the IR signals of the LbL coating increase as a function of BL numbers (Figure 2b and c). The most intense peaks are found in the 1200-400 cm^{-1} region and are mainly ascribed to Si-O stretching in both MMT and OAPOSS as well as Si-O-Al/Si-O-Si bending vibrations (Figure 2b). While MMT signals overlaps with OAPOSS ones in the 1200-1000 cm^{-1} range, the inclusion of the positively charged component within the coating is clearly pointed out by the signals associated to NH_3^+ asymmetric and symmetric stretching vibrations found in the 1800-1400 cm^{-1} region (Figure 2c). Furthermore, it is worth pointing out that these latter signals are shifted towards higher wavenumbers with respects of pure OAPOSS (*compare* Figure S1 and Figure 2c) as a consequence of the ionic interactions established with the negatively charged surface of MMT. This latter finding further proves the occurrence of the LbL assembly trough electrostatic interactions. Figure 2d reports the intensity of the peak at 1043 cm^{-1} resulting from the contribution of both OAPOSS and MMT in the assembly as function of BL number. A linear growth is found for the system deposited without salt addition in accordance with previous studies dealing with other LbL coatings containing MMT. [43] On the other hand, when the ionic strength is modified with the inclusion of 0.10 and 0.05M NaCl the growth regime of the assembly shifts from linear to supra-linear with significantly higher absorption signals. By evaluating the intensity change of signals characteristic of selected components it is possible to evaluate the effects of different ionic strength on the assembly of OAPOSS and MMT. Indeed, by comparing the NH_3^+ and Si-O-Al signals from Figure 2 c it is apparent that the change in ionic strength mainly affects the deposition of MMT. Furthermore, XRD measurements have been exploited in order to evaluate possible changes in MMT interlayer distances in the deposited LbL assembly (Figure S2). Neat MMT powder yielded a characteristic peak at $2\theta \approx 7.1°$, assigned to the

basal spacing in between each nanoplatelet. LbL assembled coatings showed a shift of this peak towards lower angles ($2\theta \approx 5°$) thus indicating a slightly increased interlayer distance. Similar results have been already discussed in the literature for other MMT containing LbL assemblies and correlated with the coating structure. [21] Indeed, the presence of such small shift has been associated to the hydrated state of MMT and correlate to a lamellar stacking process during the MMT adsorption step. [21] Moreover, the evaluation of the signal intensity clearly indicates that the inclusion of 0.10M NaCl can favor a faster lamellar staking during the deposition allowing for the built up of thicker clay stacks. The performed analyses evidence that by increasing the ionic strength of the solutions, it is possible to increase the amount of OAPOSS and, most importantly, MMT deposited at each step. The inclusion of 0.10M NaCl provides the fastest growing conditions; thus, this system, along with the unmodified one, has been chosen for the coating deposition on PET fabrics.

Coating characterization on PET fabrics

The coatings selected during the preliminary growth study on Si substrates have been then deposited onto PET fabrics. The changes in surface morphology and surface chemical composition of unmodified and LbL-coated fabrics have been evaluated by means of FE-SEM and FT-IR ATR analyses, respectively. Figure 3 reports representative micrographs and corresponding spectra.

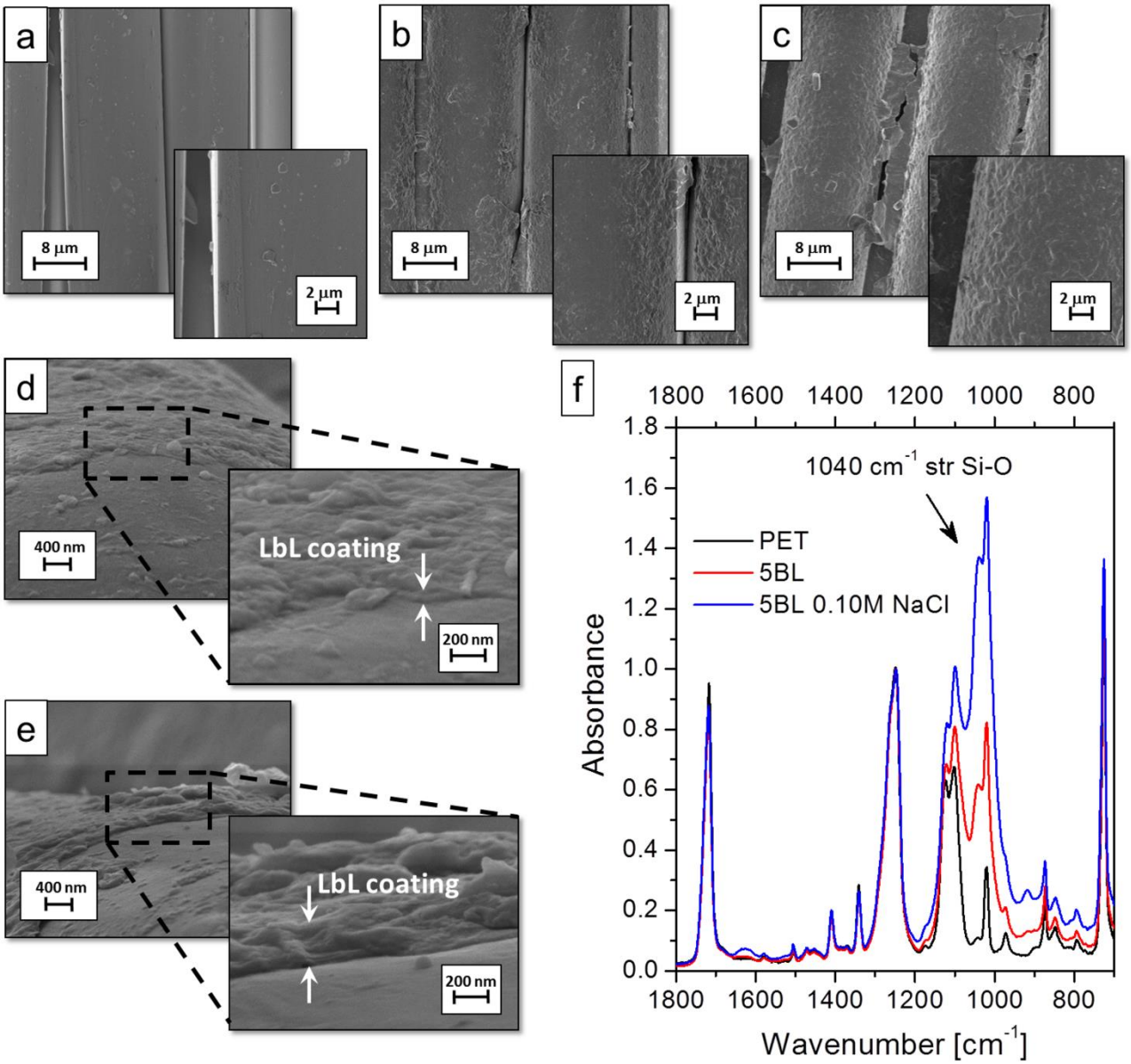

Figure 3. FE-SEM micrographs of unmodified and LbL-treated PET fabrics: neat PET (a), 5 BL (b), and 5 BL 0.10M NaCl (c); coating cross-section on 5 BL (d) and 5 BL 0.10M NaCl (e) and ATR spectra(f).

Unmodified PET fabrics show a regular and smooth surface typical of synthetic fibers (Figure 3a). When the fabrics are LbL-treated a clear change in surface morphology can be easily detected; the presence of the coating is evidenced by an increased roughness (Figures 3b and 3c), mainly ascribed to staked MMT nanoplatelets. As reported in Figure 3, the LbL deposition was found able to cover the surface of PET fibers to some extent regardless of the adopted ionic strength. However, only the deposition at 0.10M NaCl results in a homogeneous fiber coverage, (*compare* Figures 3b and 3c). Cross-section micrographs further point out the difference in thickness between the two systems;

indeed, from Figures 3d and 3e, it is apparent that the coating built at higher ionic strength is the thicker one. This is also confirmed by ATR spectra (Figure 3f) where the signal ascribed to Si-O stretching vibration is more intense for 5 BL 0.10M NaCl. From the collected characterization, it is possible to conclude that both systems can efficiently cover the surface of PET fibers and yield a homogeneous coating after the deposition of 5 BL. As demonstrated by the preliminary study on model Si wafer surface, the increase of ionic strength results in the deposition of a thicker coating also on PET fabrics. This latter finding is important as it demonstrates that the high deformation imparted to the coating during the padding processes do not compromise its stability. The add-on evaluated by weighting the fabrics before and after the LbL deposition was found to be 1.2% and 2% wt. for 5 BL and 5 BL 0.10M NaCl, respectively. As a consequence of the LbL deposition and the formation of bridges in between the fibers as reported in Figure 3 b and c, the fabrics slightly increase their stiffness.

A small preliminary durability test has been performed on LbL samples treated at high ionic strength. The aim is to evaluate whether the coating is capable of withstanding a simple washing cycle without being damaged or losing its properties. Such preliminary evaluation is important as washing stability is commonly recognized as one of the major drawbacks of LbL coatings. Thus, obtaining preliminary information concerning the intrinsic stability of the coating would allow a better design of crosslinking strategies capable of further improving it. To this aim, samples have been washed at 70°C for 1 h under vigorous stirring and then subjected to horizontal flame spread tests. Figure S3 reports a comparison between FE-SEM micrographs performed before and after the washing procedure. Interestingly, FE-SEM observations revealed no apparent damages to the coating morphology thus demonstrating that the deposited coating can survive a washing step without losing adhesion. Such finding is encouraging as it points out that the deposited LbL coatings have an intrinsic stability which is likely ascribed to the nanoscale electrostatic interactions that holds the coating components together as well as the barrier effect exerted by the highly aligned

clay platelets. This latter barrier can prevent water diffusion inside the coating thus reducing its swelling that combined with the high temperature and mechanical shear would normally wear it off. Another possible contribution to the coating stability is represented by the presence of a surface activation layer made of B-PEI. Indeed, B-PEI adsorption is considered very stable and this polyelectrolyte is often employed as anchoring layer in order to promote the coating adhesion and stability. [44] In addition, it is important to mention that washed fabrics completely regained they original hand. This is due to the rupture of the bridges joining adjacent fibers as a consequence of fibers relative movements during the washing procedure (compare Figure S3 a and b).

Thermal characterization

The thermal and thermo-oxidative stability of untreated and LbL-treated PET fabrics were investigated by TGA. The aim is to obtain fundamental degradation information useful for the interpretation of possible effects of the LbL coating on the decomposition pathways of PET. Figure S4 shows the plots for weight (TG) and derivative weight (dTG) as a function of temperature in nitrogen and air atmosphere while Table S1 collects temperature and weight data obtained from these analyses. In nitrogen, the thermal decomposition of PET takes place in a single step between 400 and 500°C and is the result of two competitive processes, namely volatilization and charring; this latter yields a final residue of 13.6%. [45] The deposition of a LbL coating does not modify the thermal decomposition of PET that still occurs in one step (Figure S4a). However, the presence of LbL-stratified MMT nanoplatelets improves the char production, as pointed out by residue values at 800°C in Table S1. It is worth mentioning that such increase is higher that the calculated coating add-on (1.2 and 2.0 wt% for 5 BL and 5 BL 0.10M NaCl, respectively) and thus has to be related to an improved PET char production. The more homogenous and thicker coating of 5 BL 0.10M NaCl yields the highest final residue and increases the PET char yield by 43%.

In air, the thermal degradation of neat PET follows two steps (Figure S4b). The first occurs between 400 and 500°C and is due to the decomposition of PET chains into smaller fragments with the

production of a carbonaceous char. [46] The second weight loss step takes place after 500°C and is related to the oxidation of the previously produced char into volatile products.[47] For coated PET, the first degradation step occurs at higher temperature and at lower degradation rates as demonstrated by T_{max1} values in Table S1 and a reduced height of the dTG curve in Figure S4b. As observed in nitrogen atmosphere, the coating improves the PET char production that is increased to 20% with respect to the 10% of untreated PET. During the second degradation step, the produced residue appears to be more thermally stable as its oxidation is shifted to higher temperatures (*see* T_{max2} values in Table S1). Such behavior can be ascribed to the preferentially oriented MMT nanoplatelets that can provide a barrier towards oxygen diffusion during both degradation steps. This slows down all reactions which depend on oxygen availability and is more apparent for 5 BL 0.10M NaCl. The final residue is 4.1 and 6.1% for 5 BL for 5 BL 0.10M NaCl, respectively; these values indicate that a small portion of organic and thermally stable residue is still present at 700°C.

Horizontal flame spread tests and cone calorimetry

The FR properties of coated fabrics have been evaluated by from flammability test (*i.e.* the reaction to a flame application) and cone calorimetry (*i.e.* the reaction to the exposure to a heat flux). Figure 4 reports the main parameters of the two tests and a schematization of the proposed flame retardant mechanism.

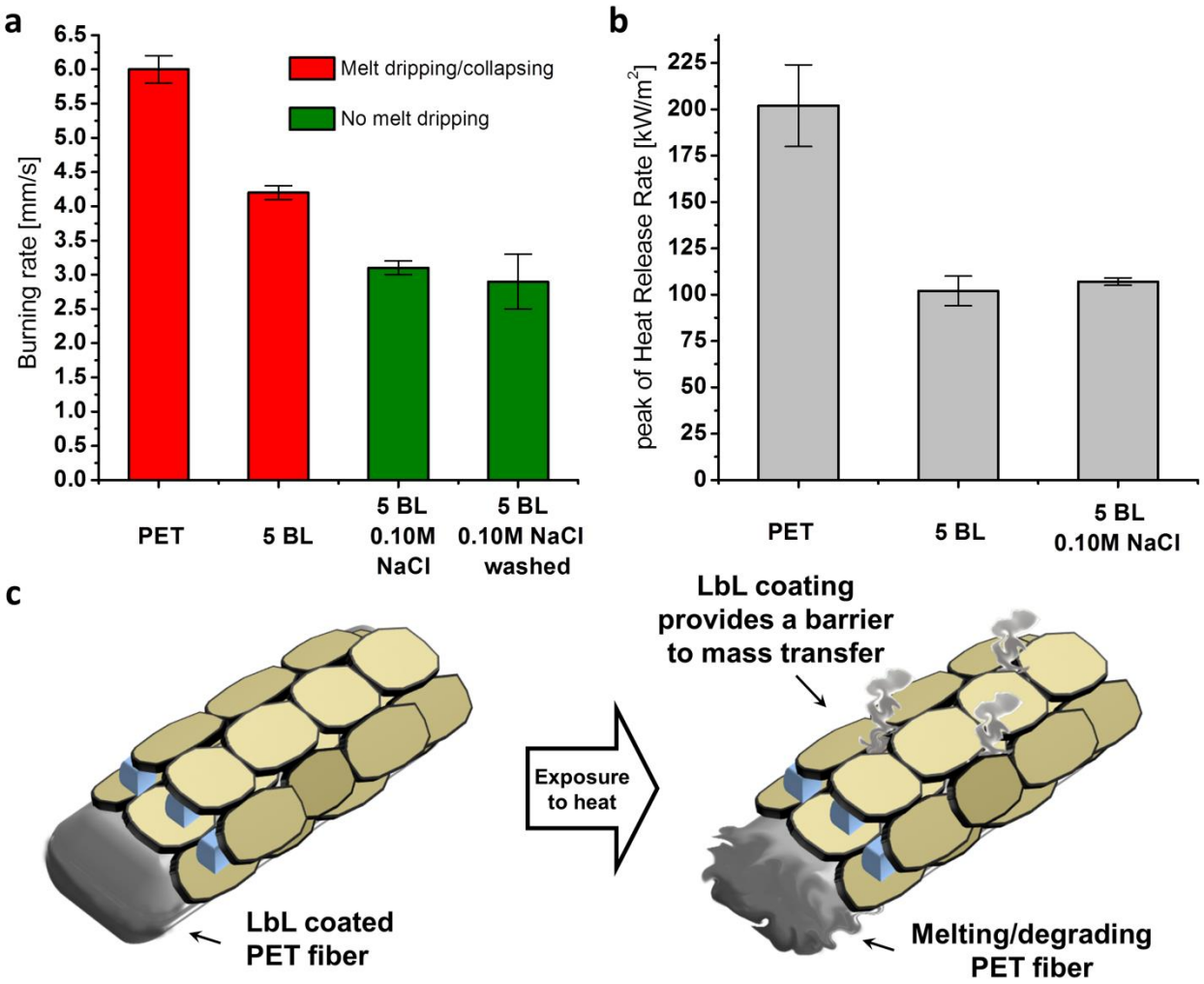

Figure 4. Main parameters of flammability and cone calorimetry tests: a) burning rates and occurrence of melt-dripping phenomenon, b) peak of Heat Release rate and c) schematization of the coating flame retardant mechanism.

The flammability test is very important as it evaluates the propensity of the fabric to initiate or propagate the fire when exposed to a small flame. The detailed test results are summarized in Table S2 while Figure S5 reports the snapshots of the samples taken during the tests. After being exposed to the small flame, the unmodified PET ignites and then crumples and loses its shape as the flame propagates along the specimen. During the combustion, some flaming droplets are released, causing the flames to dwindle and rapidly regrow while propagating on the fabric (*see* Figure S5). The

flaming droplets were always able to ignite the cotton placed underneath the sample holder. Sometimes, a vigorous dripping extinguished the flame prior to the complete combustion of the sample: for this reason the values of the final residues are highly variable (*see* Table S2). It is important to point out that although as a consequence of the melt dripping phenomenon the flame extinguishes, such behavior is highly undesirable as it can easily spread the fire to other ignitable materials in a real fire scenario, thus representing one of the most severe fire threats of PET fabrics. LbL-coated specimens showed a significantly different behavior: after the removal of the ignition source, the flame slowly and constantly propagates on the sample without the formation of molten polymer droplets. In details, 5 BL samples do not exhibit melt dripping but rather a collapsing behavior with relatively big parts of the sample detaching from the fabric and falling down igniting the cotton. This was observed for 1 out of 5 of tested samples. On the other hand, 5 BL 0.10M NaCl samples can completely suppress the melt dripping phenomenon while achieving the lowest burning rates (Figure 4a). Nearly identical performances have been registered for washed samples, further demonstrating the ability of the deposited coatings to withstand washing while maintaining the achieved flame retardant characteristics. These improvements are ascribed to the presence of the coating that can reduce the volatiles mass flow, slowing down the combustion and, on the other hand, mechanically sustain the fibers thus preventing melt dripping. This flame retardant effect shows a dependency on the coating morphology as it occurs systematically only for 5 BL 0.10M NaCl samples which are characterized by the thicker and more homogeneous deposition (*see* Figures 3d and 3f). In order to provide complementary information, cone calorimetry analyses have been performed. Cone calorimetry is a useful technique for investigating the forced combustion behavior of a material when exposed to a heat flux typical of developing fires (the 35kW/m^2 adopted here represents the initial stage of a fire). [48] During the test, the samples are quickly heated by a radiant heating source. The exposure to the heat flux triggers the thermal decomposition reactions of the polymer with subsequent release of volatile and combustible species. When a sufficient concentration is reached, such volatiles are ignited by a spark igniter and the flaming

combustion of the sample begins. The instrument measures the heat released based on the principle of that the net heat of combustion is proportional to the mass of oxygen required for combustion. Figure 4b reports one of the most commonly used flame retardant parameters, the peak of Heat Release Rate (pkHRR). The heat release rate (HRR) plots vs time are reported in Figure S6 and the collected results are summarized in Table S3. Unmodified PET fabrics ignite after an average 106 s burning with a vigorous flame, leading to a maximum HRR of 202 kW/m^2. The presence of the LbL coating, regardless of the adopted ionic strength, strongly modifies the burning behavior of the PET as reported in Figure S6. Indeed, all LbL treated samples showed an anticipation in TTI values that are reduced by 53%. However, the heat release rate is strongly reduced as demonstrated by pkHRR values reported in Table S3 (202 *vs*. 102 and 107 kW/m^2 for PET, 5 BL and 5 BL 0.10M NaCl, respectively). A similar behavior has been reported before for clay nanocomposites and, although some explanations have been proposed, the complete understanding of this phenomenon is not yet available. [49] However, besides TTI anticipation, what is currently consolidated is that the presence of clay can substantially reduce the combustion kinetics. [50] This effect has been related to the build-up of an inorganic barrier made of nanoplatelets preferentially lying flat on the surface of the burning material. As a consequence, the mass transfer that from the bulk feeds the flame with flammable volatiles is limited. [50] A similar behavior is expected to control the burning behavior of LbL-treated PET fabrics as schematized in Figure 4c. Indeed, as reported in Figure 3, each fiber is conformably coated with stratified MMT nanoplatelets intercalated by OAPOSS. The deposited coating can thus exert the function of protective barrier from the very beginning of the combustion, greatly slowing down the combustion kinetics, as demonstrated by the different shape of HRR plots between unmodified and LbL-treated PET (Figure S6). This is also corroborated by the residues collected at the end of the test (Figure S7): unmodified PET yields a limited fraction of charred polymer (5% of the original mass) while LbL-treated samples show a coherent and compact residue (11% and 12 % of the initial weight for 5 BL and 5 BL 0.10M NaCl, respectively). THR values are almost unchanged indicating that the deposited coatings mainly affect the combustion kinetics.

Finally, the presence of the coating does not affect the smoke production, as demonstrated by the nearly identical TSR values reported in Table S3.

Conclusions

OAPOSS and MMT have been Layer by Layer assembled on PET fabric employing a semi-industrial approach. The influence of the ionic strength employed during the deposition on the achieved flame retardancy properties has been investigated. The coating growth characterization performed by infrared spectroscopy demonstrated that the OAPOSS/MMT pair can yield a linear build up. The inclusion of NaCl in the process deeply influences the coating growth by modifying the ionic strength of the systems thus resulting in thicker coatings. Within the range of salt concentrations evaluated, 0.10M NaCl was found to promote the highest adsorption at each deposition step. The OAPOSS/MMT systems at zero and high ionic strengths were then successfully deposited on PET fabrics employing a dyeing padder in an impregnation and exhaustion process, thus demonstrating the feasibility of the LbL at modified ionic strength in a industrially-viable process. FE-SEM and ATR analyses pointed out that coatings deposited at higher ionic strength are thicker and more homogeneous. This difference in morphology played a key role in the burning behavior. Indeed, coatings deposited at 0.10M NaCl achieved the best flame retardant performances. The melt dripping was completely suppressed and the burning rate significantly reduced during horizontal flame spread tests. Very interestingly, these performances were maintained even after a washing cycle at 70°C for 1 h. This finding was also confirmed by FE-SEM observation and demonstrated that the coatings possess an inherent stability. By cone calorimetry treated fabrics confirmed a strong reduction in the combustion kinetics by nearly halving the peak of heat release rate. The flame retardancy mechanism of the coating is identified as a condensed phase action. The highly oriented MMT nanoplatelets assembled with OAPOSS can exert a barrier function slowing down the mass transfer of combustible volatiles towards the flame. The results described above clearly demonstrate that tuning the ionic strength during the LbL

deposition results in more thick and FR efficient LbL coatings. This is also evidenced by comparison with previous literature reports where LbL treated PET fabrics were not able to reach the same results in terms of flame spread rate and heat release rate reduction even with the use of a higher number of layers (16 vs 10 of this work). [51]

This paper highlights the importance of tuning the chemical parameters during the layer by layer deposition on fabrics in order to obtain an industrially sustainable process, thus enabling for a further step towards competitive, highly efficient and green fire protection solutions to be exploited and extended to several substrates.

Acknowledgements

The authors want to thank Mr. Mauro Raimondo and Mr. Fabio Cuttica for FE-SEM imaging and cone calorimetry analyses, respectively.

Founding

This research did not receive any specific grant from funding agencies in the public, commercial, or not-for-profit sectors.

Authors contributions

F. Carosio and J. Alongi conceived the experiments, F. Carosio coordinated the project, A. Di Pierro carried out the LbL deposition and part of the characterization. J. Alongi, A. Fina and G. Saracco contributed to the discussion and interpretation of the results. Manuscript was mainly written by F. Carosio and A. Di Pierro.

Supplementary material: IR spectra of neat MMT and OAPOSS, XRD spectra of neat MMT and LbL assembled coatings at different ionic strengths, FESEM micrograph fabrics treated at high ionic strengths before and after washing, TG and dTG data of uncoated and LbL-coated fabrics in nitrogen and air, flammability test data of uncoated and LbL-coated PET fabrics, HRR curves and cone calorimetry data are supplied as supplementary material.

References

[1] Aizenshtein E. Polyester fibres continue to dominate on the world textile raw materials balance sheet. Fibre chemistry. 2009;41(1):1-8.

[2] Alongi J, Ra H, Carosio F, Malucelli G. Update on flame retardant textiles: state of the art, environmental issues and innovative solutions: Smithers Rapra Technology Ltd; 2013.

[3] Birnbaum LS, Staskal DF. Brominated Flame Retardants: Cause for Concern? Environmental Health Perspectives. 2003;112(1):9-17.

[4] Xiao H, Shen L, Su Y, Barresi E, Dejong M, Hung H, et al. Atmospheric concentrations of halogenated flame retardants at two remote locations: the Canadian High Arctic and the Tibetan Plateau. Environmental pollution. 2012;161:154-161.

[5] Barcelo D, Kostianoy AG. Handbook environmental chemistry. In: Heidelberg S-VB, editor. Brominated flame retardants2011.

[6] Malucelli G, Carosio F, Alongi J, Fina A, Frache A, Camino G. Materials engineering for surface-confined flame retardancy. Mat Sci Eng R. 2014;84:1-20.

[7] Alongi J, Carosio F, Malucelli G. Current emerging techniques to impart flame retardancy to fabrics: An overview. Polym Degrad Stabil. 2014;106:138-149.

[8] Fina A, Camino G. Ignition mechanisms in polymers and polymer nanocomposites. Polymers for Advanced Technologies. 2011;22(7):1147-1155.

[9] Alongi J, Bosco F, Carosio F, Di Blasio A, Malucelli G. A new era for flame retardant materials? Mater Today. 2014;17(4):152-153.

[10] Carosio F, Di Blasio A, Alongi J, Malucelli G. Green DNA-based flame retardant coatings assembled through Layer by Layer. Polymer. 2013;54(19):5148-5153.

[11] Carosio F, Cuttica F, Di Blasio A, Alongi J, Malucelli G. Layer by layer assembly of flame retardant thin films on closed cell PET foams: Efficiency of ammonium polyphosphate versus DNA. Polymer Degradation and Stability. 2015;113:189-196.

[12] Carosio F, Negrell-Guirao C, Alongi J, David G, Camino G. All-polymer Layer by Layer coating as efficient solution to polyurethane foam flame retardancy. Eur Polym J. 2015;70:94-103.

[13] Carosio F, Alongi J. Ultra-Fast Layer-by-Layer Approach for Depositing Flame Retardant Coatings on Flexible PU Foams within Seconds. Acs Appl Mater Inter. 2016;8(10):6315-6319.

[14] Wang X, Pan Y-T, Wan J-T, Wang D-Y. An eco-friendly way to fire retardant flexible polyurethane foam: layer-by-layer assembly of fully bio-based substances. Rsc Adv. 2014;4(86):46164-46169.

[15] Carosio F, Di Blasio A, Alongi J, Malucelli G. Layer by layer nanoarchitectures for the surface protection of polycarbonate. European Polymer Journal. 2013;49(2):397-404.

[16] Apaydin K, Laachachi A, Ball V, Jimenez M, Bourbigot S, Toniazzo V, et al. Polyallylamine-montmorillonite as super flame retardant coating assemblies by layer-by layer deposition on polyamide. Polym Degrad Stabil. 2013;98(2):627-634.

[17] Galeska I, Hickey T, Moussy F, Kreutzer D, Papadimitrakopoulos F. Characterization and Biocompatibility Studies of Novel Humic Acids Based Films as Membrane Material for an Implantable Glucose Sensor. Biomacromolecules. 2001(2):7.

[18] Rao SV, Anderson KW, Bachas LG. Controlled Layer-By-Layer Immobilization of Horseradish Peroxidase. Biotechnology And Bioengineering. 1999;65(4):8.

[19] Zahr AS, Villiers Md, Pishko MV. Encapsulation of Drug Nanoparticles in Self-Assembled Macromolecular Nanoshells. Langmuir. 2005(21):8.

[20] Sukhorukov GB, Mohwald H. Multifunctional cargo systems for biotechnology. Trends in biotechnology. 2007;25(3):93-98.

[21] Carosio F, Colonna S, Fina A, Rydzek G, Hemmerle J, Jierry L, et al. Efficient Gas and Water Vapor Barrier Properties of Thin Poly(lactic acid) Packaging Films: Functionalization with Moisture Resistant Nafion and Clay Multilayers. Chem Mater. 2014;26(19):5459-5466.

[22] Billingham J, C.Breen, J.Harwood. Adsorption of polyamine, polyacrylic acid and polyethylene glycol on montmorillonite: An in situ study using ATR-FTIR. Vibrational Spectroscopy. 1997;14:15.

[23] R.K.Iler. Multilayers of Colloidal Particles. Journal of colloid and interface science. 1966;21:26.

[24] Decher G, Hong JD, Schmitt J. Buildup of ultrathin multilayer films by a self-assembly process: III. Consecutively alternating adsorption of anionic and cationic polyelectrolytes on charged surfaces. Thin Solid Films. 1992;210:5.

[25] Decher G. Fuzzy nanoassemblies: Toward layered polymeric multicomposites. Science. 1997;277(5330):1232-1237.

[26] Berndt P, Kurihara K, Kunitake T. Adsorption of poly(styrenesulfonate) onto an ammonium monolayer on mica: a surface forces study. Langmuir. 1992;8(10):2486-2490.

[27] Bergbreiter DE, Tao G, Franchina JG, Sussman L. Polyvalent Hydrogen-Bonding Functionalization of Ultrathin Hyperbranched Films on Polyethylene and Gold. Macromolecules. 2001;34(9):3018-3023.

[28] Sun J, Wu T, Liu F, Wang Z, Zhang X, Shen J. Covalently Attached Multilayer Assemblies by Sequential Adsorption of Polycationic Diazo-Resins and Polyanionic Poly(acrylic acid). Langmuir. 2000;16(10):4620-4624.

[29] Shimazaki Y, Mitsuishi M, Ito S, Yamamoto M. Preparation of the Layer-by-Layer Deposited Ultrathin Film Based on the Charge-Transfer Interaction. Langmuir. 1997;13(6):1385-1387.

[30] Multilayer Thin Films: Sequential Assembly of Nanocomposite Materials, 2nd Edition: Wiley-VCH; 2012.

[31] Carosio F, Negrell-Guirao C, Di Blasio A, Alongi J, David G, Camino G. Tunable thermal and flame response of phosphonated oligoallylamines layer by layer assemblies on cotton. Carbohydrate polymers. 2015;115:752-759.

[32] McAloney RA, Sinyor M, Dudnik V, Goh MC. Atomic force microscopy studies of salt effects on polyelectrolyte multilayer film morphology. Langmuir. 2001;17(21):6655-6663.

[33] Guin T, Krecker M, Milhorn A, Hagen DA, Stevens B, Grunlan JC. Exceptional Flame Resistance and Gas Barrier with Thick Multilayer Nanobrick Wall Thin Films. Advanced Materials Interfaces. 2015;2(11).

[34] Nolte AJ, Takane N, Hindman E, Gaynor W, Rubner MF, Cohen RE. Thin Film Thickness Gradients and Spatial Patterning via Salt Etching of Polyelectrolyte Multilayers. Macromolecules. 2007;40:8.

[35] Carosio F, Alongi J. Influence of layer by layer coatings containing octapropylammonium polyhedral oligomeric silsesquioxane and ammonium polyphosphate on the thermal stability and flammability of acrylic fabrics. J Anal Appl Pyrol. 2016;119:114-123.

[36] Cain AA, Plummer MGB, Murray SE, Bolling L, Regev O, Grunlan JC. Iron-containing, high aspect ratio clay as nanoarmor that imparts substantial thermal/flame protection to polyurethane with a single electrostatically-deposited bilayer. J Mater Chem A. 2014;2(41):17609-17617.

[37] Hoogeveen NG, Cohen Stuart MA, Fleer GJ, Böhmer MR. Formation and stability of multilayers of polyelectrolytes. Langmuir. 1996;12(15):3675-3681.

[38] Carosio F, Alongi J. Few durable layers suppress cotton combustion due to the joint combination of layer by layer assembly and UV-curing. Rsc Adv. 2015;5(87):71482-71490.

[39] Tata J, Alongi J, Carosio F, Frache A. Optimization of the procedure to burn textile fabrics by cone calorimeter: Part I. Combustion behavior of polyester. Fire Mater. 2011;35(6):397-409.

[40] Zhang Z, Liang G, Lu T. Synthesis and characterization of cage octa (aminopropylsilsesquioxane). J Appl Polym Sci. 2007;103(4):2608-2614.

[41] Socrates G. Infrared and Raman Characteristic Group Frequencies New York: Wiley; 2004.

[42] Madejová J. FTIR techniques in clay mineral studies. Vibrational spectroscopy. 2003;31(1):1-10.

[43] Laufer G, Kirkland C, Cain AA, Grunlan JC. Clay-Chitosan Nanobrick Walls: Completely Renewable Gas Barrier and Flame-Retardant Nanocoatings. Acs Appl Mater Inter. 2012;4(3):1643-1649.

[44] Szilagyi I, Trefalt G, Tiraferri A, Maroni P, Borkovec M. Polyelectrolyte adsorption, interparticle forces, and colloidal aggregation. Soft Matter. 2014;10(15):2479-2502.

[45] Alongi J, Camino G, Malucelli G. Heating rate effect on char yield from cotton, poly(ethylene terephthalate) and blend fabrics. Carbohydrate polymers. 2013;92(2):1327-1334.

[46] Martın-Gullon I, Esperanza M, Font R. Kinetic model for the pyrolysis and combustion of poly-(ethylene terephthalate)(PET). J Anal Appl Pyrol. 2001;58:635-650.

[47] Wang X-S, Li X-G, Yan D. Thermal decomposition kinetics of poly (trimethylene terephthalate). Polym Degrad Stabil. 2000;69(3):361-372.

[48] Schartel B, Hull TR. Development of fire-retarded materials—Interpretation of cone calorimeter data. Fire Mater. 2007;31(5):327-354.

[49] Fina A, Cuttica F, Camino G. Ignition of polypropylene/montmorillonite nanocomposites. Polym Degrad Stabil. 2012;97(12):2619-2626.

[50] Kiliaris P, Papaspyrides C. Polymer/layered silicate (clay) nanocomposites: an overview of flame retardancy. Prog Polym Sci. 2010;35(7):902-958.

[51] Pan Y, Wang W, Pan H, Zhan J, Hu Y. Fabrication of montmorillonite and titanate nanotube based coatings via layer-by-layer self-assembly method to enhance the thermal stability, flame retardancy and ultraviolet protection of polyethylene terephthalate (PET) fabric. Rsc Adv. 2016;6(59):53625-53634.